Supplementary Data

for

Red blood cells contain enzymatically active GPx4 whose abundance anticorrelates with hemolysis during blood bank storage

In *Redox Biology*

https://doi.org/10.1016/j.redox.2021.102073

July 2021

Jeffrey M. Stolwijk[1,2*], Jonathan A. Stefely[3,4*], Mike T. Veling[5,6], Thomas J. van 't Erve[1,2], Brett A. Wagner[1], Thomas J. Raife[3**] and Garry R. Buettner[1**],

[1]Free Radical and Radiation Biology Program, The University of Iowa Carver College of Medicine, Iowa City, IA, USA.
[2]Interdisciplinary Graduate Program in Human Toxicology, The University of Iowa, Iowa City, IA, USA.
[3]Department of Pathology and Laboratory Medicine, School of Medicine and Public Health, University of Wisconsin–Madison, Madison, WI, USA.
[4]Medical Scientist Training Program, School of Medicine and Public Health, University of Wisconsin–Madison, Madison, WI, USA.
[5]Department of Systems Biology, Harvard Medical School, Boston, MA, USA.
[6]Wyss Institute for Biologically Inspired Engineering, Harvard University, Boston, MA, USA.
*These authors contributed equally to this work
**Corresponding authors: Garry-Buettner@uiowa.edu ; TRaife@uwhealth.org

Table of Contents

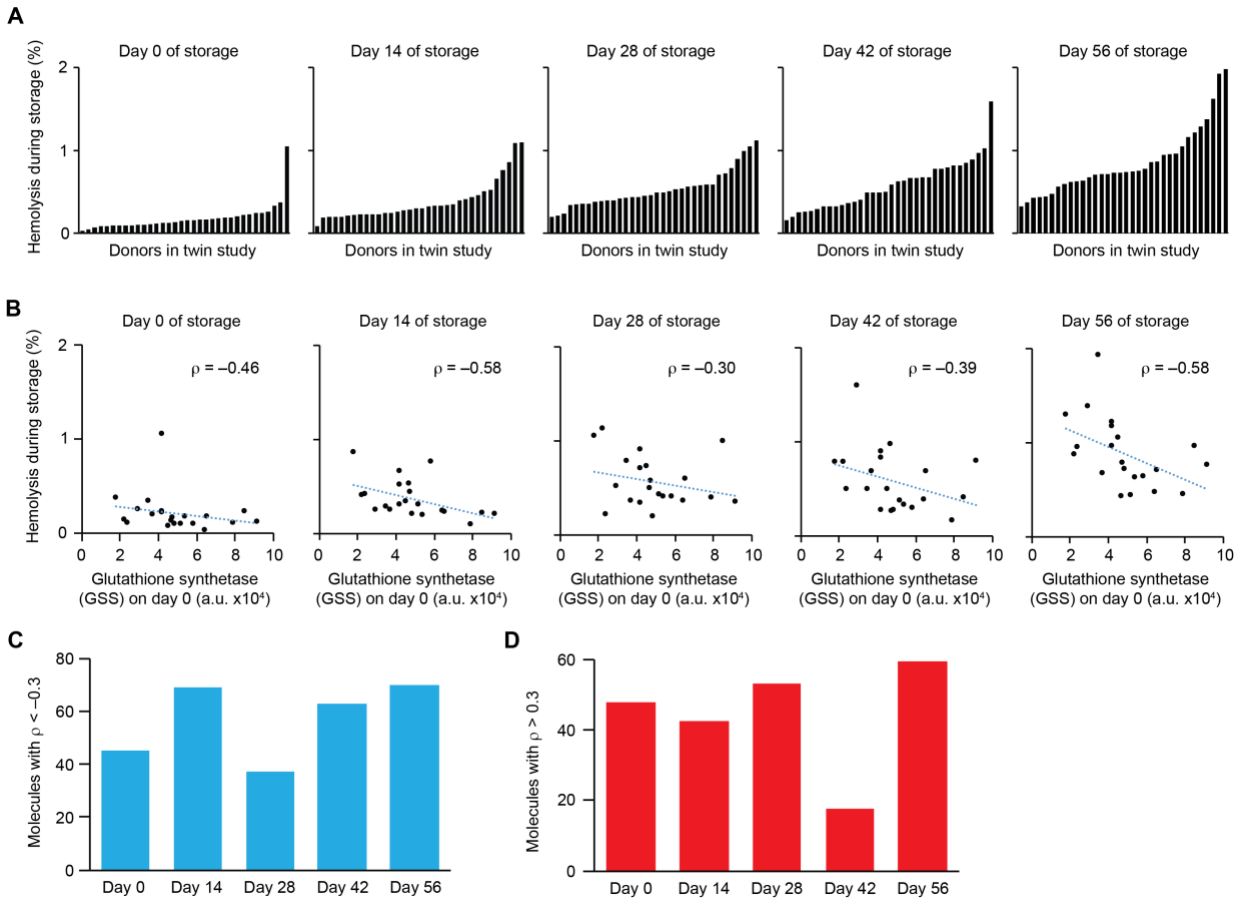

Figure S1. Rates of hemolysis of RBCs varies depending on the donor and time.

(A) RBC hemolysis (%) across all of the donors in the twin study at each of the five time points in the study. Raw data from [1].

(B) Scatter plots of RBC hemolysis at variable days of storage (%) *vs.* the abundance of the protein glutathione synthetase (GSS).

(C) Number of molecules anti-correlated with hemolysis ($\rho < -0.3$) at each of the time points in the study.

(D) Number of molecules correlated with hemolysis ($\rho > 0.3$) at each of the time points in the study.

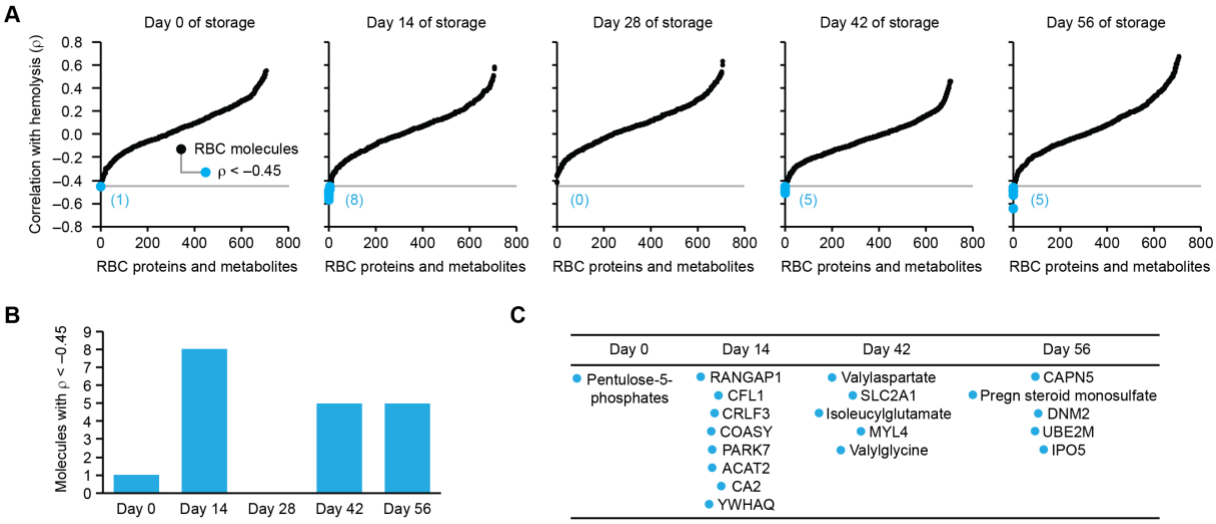

Figure S2. RBC molecules that correlate with hemolysis vary depending on the time point.

(A) Rank order plots of RBC molecules (proteins and metabolites) correlated with hemolysis at each of the time points shown. Correlations are quantified as Spearman's rank correlation coefficients (ρ). Blue points and the numbers in parentheses indicate molecules with $\rho < -0.45$.

(B) Number of molecules strongly anti-correlated with hemolysis ($\rho < -0.45$) at each of the time points in the study.

(C) Table of the molecules strongly anti-correlated with hemolysis ($\rho < -0.45$) at each of the time points in the study.

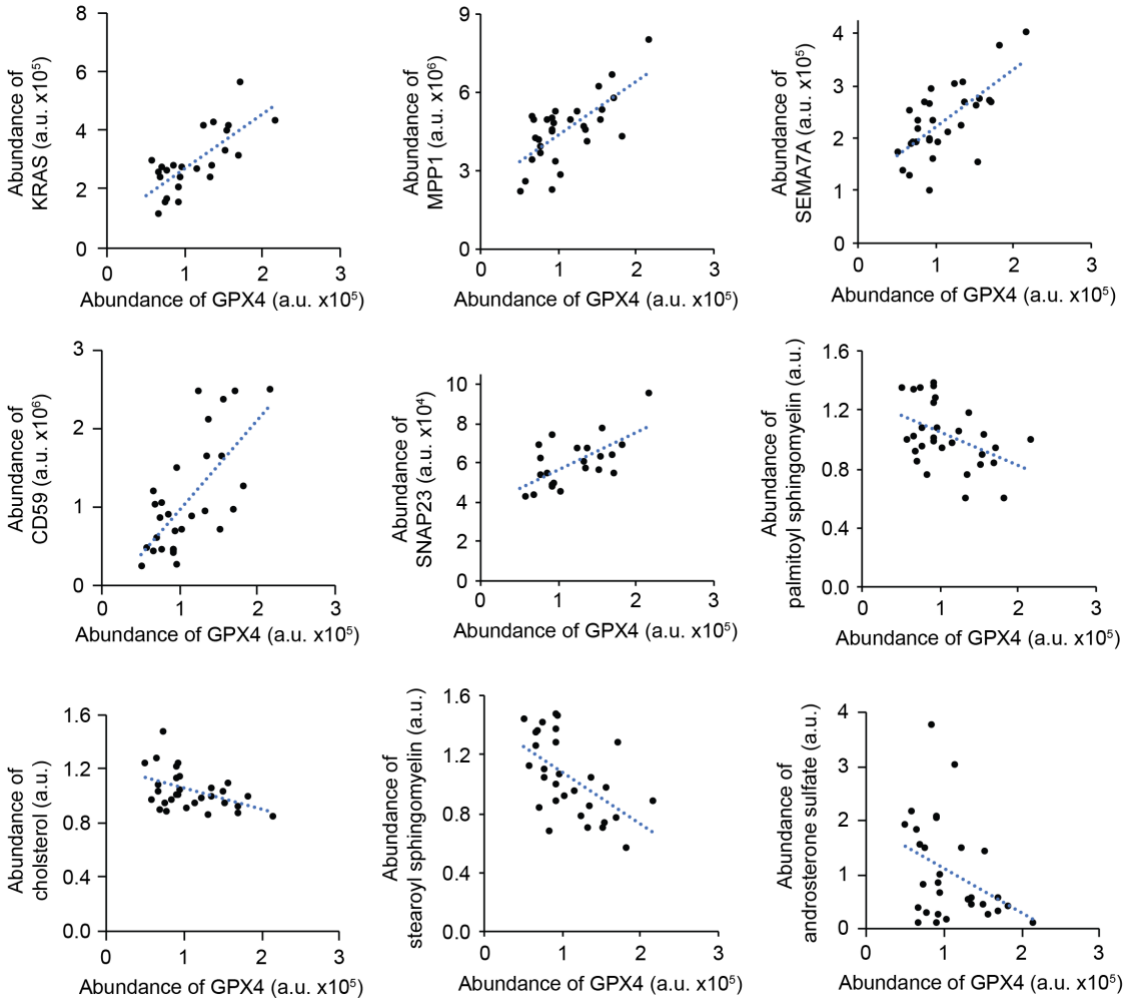

Figure S3. Select RBC molecules correlated or anti-correlated with GPx4.

Scatter plots of a sub-set of the RBC molecules correlated or anti-correlated with GPx4.

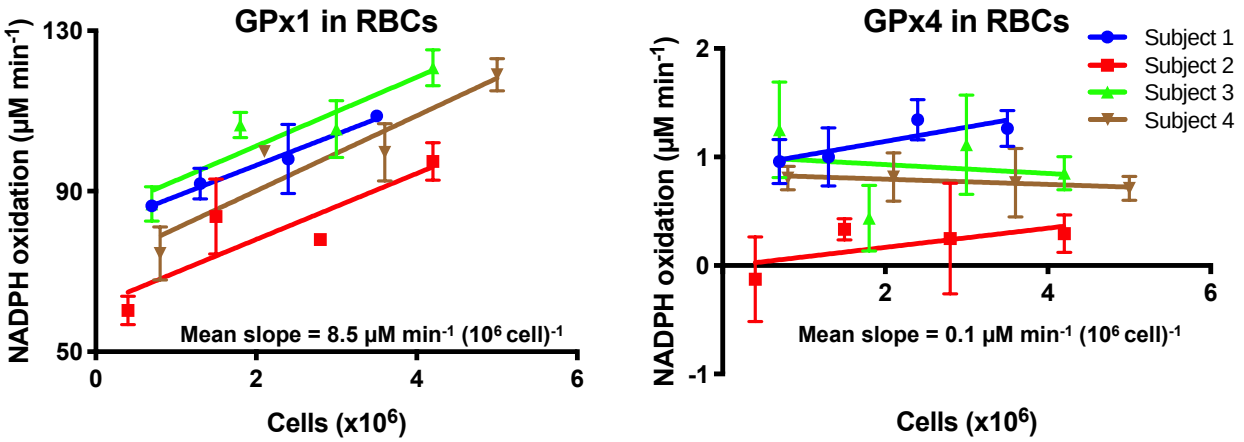

Figure S4. GPx1 and GPx4 activity in RBCs.

For each subject, activities for both GPx1 and GPx4 were determined with an increasing number of cells in the sample. The ordinate for each panel represents the rate of oxidation of NADPH; this rate is a linear function of the number of cells in the sample and the amount of active GPx in the cells. Note that the slopes for the GPx4 assay for subjects #1 and #2 are only about 1% of the slopes from the corresponding GPx1 assays, indicating that the amount of GPx4 in RBCs is considerably less than GPx1. This observation is consistent with the data on the proteome of RBCs in which the copy number for GPx4 is about 5% of that of GPx1 [2]. The negative slopes for GPx4 for subjects #3 and #4 were determined to be due to the interference of the Soret band from small amounts of contaminating hemoglobin. Small amounts of contaminating hemoglobin do not interfere with the assay for GPx1 because of its much greater abundance; it is essential to minimize contaminating hemoglobin as much as possible to optimally detect GPx4 activity in this assay. The subjects, #1 – #4, in this figure are different from the subjects A – D in Figure 3.

Description of Supplementary Data Sets

Supplementary Data Set 1. Compiled Donor Twin Study RBC Data Set

Integrated table of RBC hemolysis measurements (at days 0, 14, 28, 42, and 56 of storage), RBC protein abundance measurements (at day 0 of storage), RBC metabolite abundance measurements (at day 0 of storage), and heritability estimates in the twin study. The first four columns include identifiers for the metabolites, proteins, or time points at which hemolysis was measured. The fifth column includes heritability measurements, where available as previously described, based on ref [3] (for proteins and metabolites) or ref [1] (for hemolysis). The remaining columns include protein abundance (raw data from ref [3]), metabolite abundance (raw data from ref [3]), or hemolysis (raw data from ref [1]) measurements for each RBC unit in the twin study. These columns are labeled as "RBC Unit #n", where "n" denotes a study-specific reference number for the individual donor in the twin study. (This file was generated by Microsoft® Excel for Mac, Version 16.16.13 (190811).)

Supplementary Data Set 2. RBC molecule-hemolysis correlations

Table of Spearman's rank correlation coefficients (Rho) between RBC molecule abundances and hemolysis measurements. The first four columns include identifiers for the metabolites and proteins. The fifth column includes heritability measurements, where available, as previously described [3]. The remaining columns include individual Spearman's rank correlation coefficients (Rho) for pairwise molecule-hemolysis correlations. Positive values indicate correlations, and negative values indicate anti-correlations. Correlations were determined for hemolysis at each individual time point (days 0, 14, 28, 42, and 56 of storage) and for the rate of RBC hemolysis across time points. The first tab of the spreadsheet includes correlations only for molecules with at least 18 protein abundance measurements (at least 18 out of the total 34 possible in the data set). The second tab includes the full set of correlations determined, regardless of the number of underlying data points. The third tab contains a table of the number of data points underlying each correlation coefficient determination (*n*). (This file was generated by Microsoft® Excel for Mac, Version 16.16.13 (190811).)

Supplementary Data Set 3. Heritable RBC molecule-hemolysis correlations

Table of Spearman's rank correlation coefficients (Rho) between RBC molecule abundances and hemolysis measurements—only for molecules for which a heritability estimate was determined [3]. The first four columns include identifiers for the metabolites and proteins. The fifth column includes heritability measurements [3]. The remaining columns include individual Spearman's rank correlation coefficients (Rho) for pairwise molecule-hemolysis correlations. Positive values indicate correlations, and negative values indicate anti-correlations. These correlations were determined for hemolysis at each individual time point (days 0, 14, 28, 42, and 56 of storage) and for the rate of RBC hemolysis across time points. The first tab includes all correlation coefficients, and reflects the data shown in **Figure 2A**. The second tab includes only molecules with a Spearman's $\rho < -0.3$ at the day 14 time point, and reflects the data shown in **Figure 2B**. (This file was generated by Microsoft® Excel for Mac, Version 16.16.13 (190811).)

Supplementary Data Set 4. Gene Ontology (GO) sets enriched in anti-correlated proteins

Table of Gene Ontology (GO) categories significantly ($P < 0.05$) enriched in proteins anti-correlated with hemolysis ($n = 33$), as defined by Rho < –0.3, compared to all RBC proteins with measured heritability ($n = 385$). The first tab includes the GO categories, the proteins in these GO categories, the total number of proteins for each GO category present in the full set of heritable proteins, the total number these proteins that are anti-correlated with hemolysis, the enrichment score, the *P*-value, and the false discovery rate (FDR). The second tab includes the set of proteins anti-correlated with hemolysis ($n = 33$), as defined by Rho < –0.3. The third tab includes the full set RBC proteins with measured heritability ($n = 385$). (This file was generated by Microsoft® Excel for Mac, Version 16.16.13 (190811).)

Supplementary Data Set 5. RBC molecule-molecule correlations in the twin study data set

Matrix of molecule-molecule correlations (abundance *vs*. abundance) (Pearson correlation coefficients)—only for molecules for which a heritability was able to be determined based on ref [3]. The first tab includes the full matrix of Pearson correlation coefficients for these molecules. The second tab includes Pearson correlation coefficients for correlations with the abundance of GPx4 only (corresponding to **Figure 3C**). The third tab includes the underlying data set (molecule abundance measurements) used to generate the molecule-molecule correlation matrix. (This file was generated by Microsoft® Excel for Mac, Version 16.16.13 (190811)).

Extended Materials and Methods

Optimizing the assay for GPx activity in human erythrocytes

To further validate our ability to measure GPx4 activity in human RBCs, the following experiment was undertaken: Whole blood was collected from 4 subjects in heparin tubes. A portion of the packed RBCs (2000 ***g***, 20 min) was aspirated, avoiding the buffy coat. Then, the RBCs were washed and counted. The RBC suspension was further diluted to generate samples consisting of (0.5 – 5) x 10^6 cells. This is crucial to replicate the linearity of activity *i.e.* more cells yield more activity, **Figure S4**. The packed RBCs were resuspended in Tris-Base (0.10 M, pH 8.0) containing EDTA, NaN_3 (2.0 mM, 1.5 mM). 0.1% Triton X-100. Because RBCs have considerable GPx1 activity, four samples per dilution were used to measure GPx1 activity. The raw activity in μM NADPH oxidized min^{-1}, was then plotted *vs.* the number of cells in the assay. All plots appear linear and are positive, indicating GPx1 activity is being measured.

A similar design was used to determine the linearity of GPx4. The GPx4 assay results for RBC samples from subjects #1 and #2 are linear with a positive slope, as expected. However, samples from subjects #3 and #4 presented with slightly negative slopes, indicating some sort of interference. This interference was determined to be due to the Soret band of the small amount of contaminating hemoglobin present in these samples. For subjects #3 and #4 these same small amounts of contaminating hemoglobin do not interfere with the assay for GPx1, because of its much greater abundance. It is essential to minimize as much as possible contaminating hemoglobin to have success with the GPx4 activity assay. The results for subjects #3 and #4 are presented in **Figure S4** only as examples of samples that cannot be analyzed to yield valid results for the activity of GPx4 due to hemoglobin interference.

Kinetic considerations to compare results from the combination GPx1-GPx4 assay

In the combination assay for GPx1 and GPx4, the definition of Units of activity are the same for both enzymes. In accordance with the International Units for Enzymes we report the activities of GPx1 and GPx4 as: 1 Unit (U) is the amount of enzyme that catalyzes the conversion of 1 μmole of substrate per minute [4]. However, although the overall kinetic mechanism for the removal of their respective substrates are identical [5], the rate constants of the various steps appear to be somewhat different; also, in the assay the concentration of the hydroperoxide substrates are different. Thus, in the assay the amount of enzyme that produces one Unit of activity are likely to be somewhat different for GPx1 and GPx4.

A simple overview of the reaction mechanism for the removal of hydroperoxides by GPx1 and GPx4 is:

$$GPx_{reduced} + ROOH + H^+ \xrightarrow{k_1} GPx\text{-}OH + ROH \quad (1)$$

$$GPx\text{-}OH + GS^- + H^+ \xrightarrow{k_2} GPx\text{-}SG + H_2O \quad (2)$$

$$GPx\text{-}SG + GS^- \xrightarrow{k_3} GPx_{reduced} + GSSG \quad (3)$$

A much more detailed mechanism is provided in [6, 7].

Table S1 provides kinetic parameters for GPx1 and GPx4 for comparison.

Table S1. Key aspects of the kinetics of the combination assay.

	GPx1	GPx4	Ref
k_1	4×10^7 M^{-1} s^{-1} [a,b]	1×10^7 M^{-1} s^{-1} [c]	[8]
k_2	2×10^5 M^{-1} s^{-1} [a,d]	0.5×10^5 M^{-1} s^{-1} [c]	[8]
$[H_2O_2]$	260 μM [e]	NA[e]	
PL-OOH	NA[e]	30 μM [e]	

[a] Rate constant for the removal of H_2O_2 determined in aqueous solution with 2 mM GSH, 60 μM peroxide, pH 7.4, at 37 °C; these rate constants would be somewhat greater at pH 8.0, the pH of the combination assay [9].

[b] This rate constant is for tetrameric GPx1. The monomeric rate constant will be about 1×10^7 M^{-1} s^{-1}, similar to GPx4, which is a monomer.

[c] Rate constant for the removal of PC-OOH determined in aqueous solution with 2 mM GSH, 60 μM peroxide, pH 7.4, 0.1% Triton X-100 and 0.24 mM sodium deoxycholate at 37 °C; these rate constants would be somewhat greater at pH 8.0, the pH of the combination assay [9].

[d] This rate constant is for tetrameric GPx1. The monomeric rate constant will be 0.5×10^5 M^{-1} s^{-1}, again similar to k_2 for GPx4, which is a monomer.

[e] Concentration in the combination assay; NA, not applicable, *i.e.* the reactivity of GPx4 is minimal with H_2O_2; likewise, the reaction of GPx1 with PCOOH is minimal in the combination assay [6, 7, 9].

The concentrations of the components of the activity assay for GPx1 and GPx4 are chosen to ensure that reaction 2 above is rate-limiting. The rate constant for reaction 3, k_3, is much greater than k_2, $k_3 \approx 10^7$ M^{-1} s^{-1} [10, 11]. Thus, in the assay k_3 has no influence on the kinetics being monitored. Note that substrate concentration for GPx1 is about 9-fold greater than for GPx4. However, for each enzyme the concentration of oxidizing substrate is much greater than the concentration of the enzyme. Thus, the enzymes are completely oxidized and the rate of removal of oxidizing substrate and the associated consumption of NADPH is controlled by k_2. However, the monomeric rate constants, k_2, for the first step in the recycling of both GPx1 and GPx4 are the same. Thus, the difference in the concentrations of oxidizing substrate will have little influence on the value of 1 Unit of activity. In the combination assay GPx1 and its substrate, H_2O_2, are homogenously distributed in the assay solution, while GPx4 and its substrate are not homogenously distributed. This clearly may have an influence, as Triton X-100 will concentrate GPx4 and PCOOH into the reaction domains generated by Triton X-100, possibly accelerating the reactions for removal of PCOOH. But even with these caveats, the observed units of activity for each enzyme are somewhat comparable and thus provide interesting information.

In the seminal study of the human red blood cell proteome of Bryk and Wiśniewski [12], it was found that the copy number of GPx1 monomers was about 20x the number of GPx4 monomers. Our kinetic considerations above provide a rationale for the difference in these two measures of GPx1 and GPx4.

Interesting is an order-of-magnitude comparison of the “concentrations” of GPx1 and GPx4 in their respective domains: Human RBCs have an overall volume of about 90 fL (90 μm^3). The surface area of RBCs is about 140 μm^2. If we assume the distance across the lipid bilayer to be about 4 nm (0.004 μm) [13], then the volume of the RBC membrane is on the order of 0.6 fL or about 1% of total cell volume. Thus, to an order-of-magnitude, the amount of enzyme in their respective domains of activity are quite similar.

References, Supplemental

1 van 't Erve TJ, Wagner BA, Martin SM, Knudson CM, Blendowski R, Keaton M, Holt T, Hess JR, Buettner GR, Ryckman KK, Darbro BW, Murray JC, Raife TJ. (2015) The heritability of hemolysis in stored human red blood cells. *Transfusion*. **55(6):**1178-1185. PMID: 25644965 http://doi.org/10.1111/trf.12992

2 Bryk AH, Wiśniewski JR. (2017) Quantitative analysis of human red blood cell proteome. *J Proteome Res.* **16(8):**2752-2761PMID: 28689405 http://doi.org/10.1021/acs.jproteome.7b00025

3 Weisenhorn EM, van 't Erve TJ, Riley NM, Hess JR, Raife TJ, Coon JJ. (2016) Multi-omics Evidence for Inheritance of Energy Pathways in Red Blood Cells. *Mol Cell Proteomics.* **15(12):**3614-3623. PMID: 27777340 https://doi.org/10.1074/mcp.M116.062349

4 Burtis CA, Geary TD. (1994) Glossary of bioanalytical nomenclature - Part 1: General terminology, body fluids, enzymology, immunology (IUPAC Recommendations 1994), *Pure Appl. Chem*. **66:**2587-2604. https://doi.org/10.1351/pac199466122587

5 Ursini F, Maiorino M, Gregolin C. (1985) The selenoenzyme phospholipid hydroperoxide glutathione peroxidase. *Biochim Biophys Acta Gen Subj*. **839**:62–70. PMID: 3978121 https://doi.org/10.1016/0304-4165(85)90182-5

6 Flohé L, Brigelius-Flohé R. (2012) Selenoproteins of the glutathione peroxidase family. pp. 167-180, Ch13 In Dolph L. Hatfield DL, Berry MJ, Vadim N, Gladyshev VN. (Editors) *Selenium: Its Molecular Biology and Role in Human Health*. Http://doi.org/10.1007/978-1-4614-1025-6_13 Springer Science

7 Maiorino M, Bosello V, Cozza G, Roveri A, Toppo S, Ursini F. (2012) Glutathione Peroxidase-4. pp 181-195, Ch 14 In Dolph L. Hatfield DL, Berry MJ, Vadim N, Gladyshev VN. (Editors) *Selenium: Its Molecular Biology and Role in Human Health*. Http://doi.org/10.1007/978-1-4614-1025-6_14 Springer Science

8 Takebe G, Yarimizu J, Saito Y, Hayashi T, Nakamura H, Yodoi J, Nagasawa S, Takahashi K. (2002) A comparative study on the hydroperoxide and thiol specificity of the glutathione peroxidase family and selenoprotein P. *J Biol Chem*. **277(43):**41254-41258. PMID: 12185074 http://doi.org/10.1074/jbc.M202773200

9 Stolwijk JM, Falls-Hubert KC, Searby CC, Wagner BA, Buettner GR (2020) Simultaneous detection of the enzyme activities of GPx1 and GPx4 guide optimization of selenium in cell biological experiments. *Redox Biology*. **32:**10158. PMID: 32278283 https://doi.org/10.1016/j.redox.2020.101518

10 Ursini F, Maiorino M, Brigelius-Flohe´ R, Aumann KD, Roveri A, Schomburg D, Flohe´ L. (1995) Diversity of glutathione peroxidases. *Methods Enzymol*. **252:**38-53. PMID: 7476373 https://doi.org/10.1016/0076-6879(95)52007-4

11 Ng CF, Schafer FQ, Buettner GR, Rodgers VGJ. (2007) The rate of cellular hydrogen peroxide removal shows dependency on GSH: Mathematical insight into in vivo H_2O_2 and GPx concentrations. *Free Rad Res.* **41:**1201-1211. PMID: 17886026 http://dx.doi.org/10.1080/10715760701625075

12 Bryk AH, Wiśniewski JR. (2017) Quantitative analysis of human red blood cell proteome. *J Proteome Res*, **16(8):**2752–2761. PMID: 28689405 http://doi.org/10.1021/acs.jproteome.7b00025

13 Geekiyanage NM, Balanant MA, Sauret E, Saha S, Flower R, Lim CT, Gu YT. (2019) A coarse-grained red blood cell membrane model to study stomatocyte-discocyte-echinocyte morphologies. *PLoS ONE.* **14(4):** e0215447. PMID: 31002688 https://doi.org/10.1371/journal.pone.0215447